

RSC Advances



This is an *Accepted Manuscript*, which has been through the Royal Society of Chemistry peer review process and has been accepted for publication.

Accepted Manuscripts are published online shortly after acceptance, before technical editing, formatting and proof reading. Using this free service, authors can make their results available to the community, in citable form, before we publish the edited article. This *Accepted Manuscript* will be replaced by the edited, formatted and paginated article as soon as this is available.

You can find more information about *Accepted Manuscripts* in the [Information for Authors](#).

Please note that technical editing may introduce minor changes to the text and/or graphics, which may alter content. The journal's standard [Terms & Conditions](#) and the [Ethical guidelines](#) still apply. In no event shall the Royal Society of Chemistry be held responsible for any errors or omissions in this *Accepted Manuscript* or any consequences arising from the use of any information it contains.

Creating Surface Patterns of Polymer Brushes by degrafting via Tetrabutyl Ammonium Fluoride

Rohan Patil¹, Douglas Kiserow^{1,2}, Jan Genzer^{1,*}

¹ Department of Chemical and Biomolecular Engineering
North Carolina State University
Raleigh North Carolina 27695-7905, USA

² US Army Research Office
Research Triangle Park, North Carolina 27709-2211, USA

Abstract

We demonstrate the use of tetrabutyl ammonium fluoride (TBAF) for creating spatial patterns of poly(methyl methacrylate) (PMMA) brushes on a flat silica support by degrafting PMMA grafted chains from selected regions on the substrate. We generate gradient in grafting density of PMMA brushes by dipping substrates featuring homogeneous PMMA brush assemblies into TBAF solution. Desired in-plane patterns in the PMMA brush layer in millimeter scale are created by using a microcontact printing TBAF with a stamp made of agarose gel. The use of TBAF for degrafting is appealing because it cleaves selectively Si-O bonds and activates hydroxyl groups on silicon surfaces to enable deposition of organosilane-based initiators for growth of a fresh polymer brush layer. The latter is verified by using ellipsometry, X-ray photoelectron spectroscopy, and water contact angle measurements. The reusability of the substrate allows us to create a diblock copolymer brushes on selected portions of the substrate not exposed to TBAF while decorating the TBAF-treated sections of the substrate with homopolymer brushes.

* Corresponding author: Jan Genzer (jan_genzer@ncsu.edu)

1. Introduction

Surface grafted polymer assemblies (SGPAs) comprise polymer chains tethered to a substrate or interface.¹⁻³ Such systems are colloquially referred to as “polymer brushes”, although the term “brush” describes correctly only a particular conformation of polymeric grafts, in which the grafted macromolecules stretch away from the substrate due to close proximity of the grafting points and excluded volume interactions. The tethered nature of the SGPAs imparts additional stability and offers the ability to control polymer conformation by changing the grafting density (σ_p), *i.e.*, the number of grafted polymer chains per unit area on the substrate. Altering the molecular weight (MW), topology and chemical composition (including sequence distribution of monomers, for the case of copolymers) enable additional fine-tuning of the brush characteristics. In addition to altering chemical composition within the individual polymer chains, some applications demand generating structures with chemical composition variation in the plane of the substrate. Creating surface patterns on thin films, specifically in regard to polymer brushes, is of immense interest due to potential applications in studying polymer brush structure⁴, protein patterning^{5,6}, protein adsorption⁷, cell adhesion^{8,9}, or stimuli-responsive surfaces.^{10,11}

Patterned brush surfaces are generated typically by two general methodologies. The first approach involves creating patterns of initiators on the substrate and then growing polymer brushes directly from the substrate-bound initiator centers. A pattern of an initiator layer is formed typically by using photolithographic or soft lithographic methods, *i.e.*, micro-contact printing¹². Alternatively, the initiator arrays may feature gradients in density^{13,14} or mixed monolayers featuring two different initiators.¹⁵ The polymer brush is grown by surface-initiated (SI) polymerization, for instance via atom transfer radical polymerization (ATRP). Previous efforts include the work of Chen *et al* on depositing patterned thiol based surface initiator on a gold substrate and growing polymer on top using SI-ATRP.¹⁶ The patterns of initiators were generated by employing PDMS stamps¹⁷ and self-assembled microspheres.¹⁸ The initiator patterns were later translated into polymer brush patterns after growing polymers using ATRP from the initiator sites on the substrate. A complimentary technique involves preparing a uniform layer of initiator and deactivating part of the layer using UV light incident across a mask.^{8,9} The second approach starts with a homogeneous polymer brush layer, which is subsequently patterned by: 1) chemically or physically altering the existing brushes (*e.g.*

irreversibly crosslinking a patterned area using UV light¹⁰), 2) growing new blocks onto predefined regions on the substrate, or by selectively removing chains from the substrate (*i.e.*, by photocleaving¹⁹). Micrometer scale chemical gradients of quaternized poly(2-dimethylaminoethyl methacrylate) (PDMAEMA) have been prepared by Koo *et al* by controlling the diffusion of alkylating agent through a PDMS channel.²⁰ Schuh *et al* created patterns on an azo functionalized poly(methacrylic acid) brush layer by photomechanical degrafting using interference patterns of light.²¹ Wei *et al* used a hybrid approach where the initiator pattern was deposited on top of a polymer brush layer and then a second polymer brush layer was grown, which amplified the initiator pattern.²²

We have demonstrated recently that poly(methyl methacrylate) (PMMA) brushes can be degrafted efficiently from silicon substrates by using tetrabutyl ammonium fluoride (TBAF).^{23,24} TBAF is a mild degrafting reagent, in comparison to others, such as HF²⁵, acids²⁶, bases²⁷ or techniques which use UV light²⁸, which could damage either the substrate or the polymer backbone. The kinetics and extent of degrafting can be controlled with high fidelity by tuning the incubation time, temperature, and concentration of TBAF. TBAF reacts selectively with the Si–O bonds present exclusively at the base of the initiator without affecting the backbone of the polymer. In this Communication we demonstrate that various polymer patterns can be created on the substrate by controlling the position and time for delivery of TBAF solution. The substrate can be reused to grow brushes multiple times. We also show that polystyrene brushes can be degrafted using TBAF followed by regrowing PMMA brushes. Partial degrafting and regrowing of brushes allows us to create regions with diblock copolymer and homogeneous polymer brushes on the same substrate.

2. Results and discussion

2.1 Creating Gradients of Polymer Brush Grafting Density using Degrafting

Degrafting of PMMA using TBAF can be controlled by 1) adjusting the incubation time of the sample in TBAF solution, 2) varying the concentration of TBAF in solution, and 3) altering the temperature of the TBAF solution. These attributes are employed in conjunction with gradual sample exposure to TBAF solution using the dipping method to create a gradient in grafting density of polymer brushes. **Figure 1** shows the thickness measured over the length of sample

before (blue squares) and after (red circles) dipping vertically in a degrafting TBAF solution for 2 different specimens. The bottom most part of the substrate (*i.e.* position 5 mm) has the lowest grafting density since it is incubated for the longest time in the TBAF solution and hence has undergone the highest degree of degrafting.

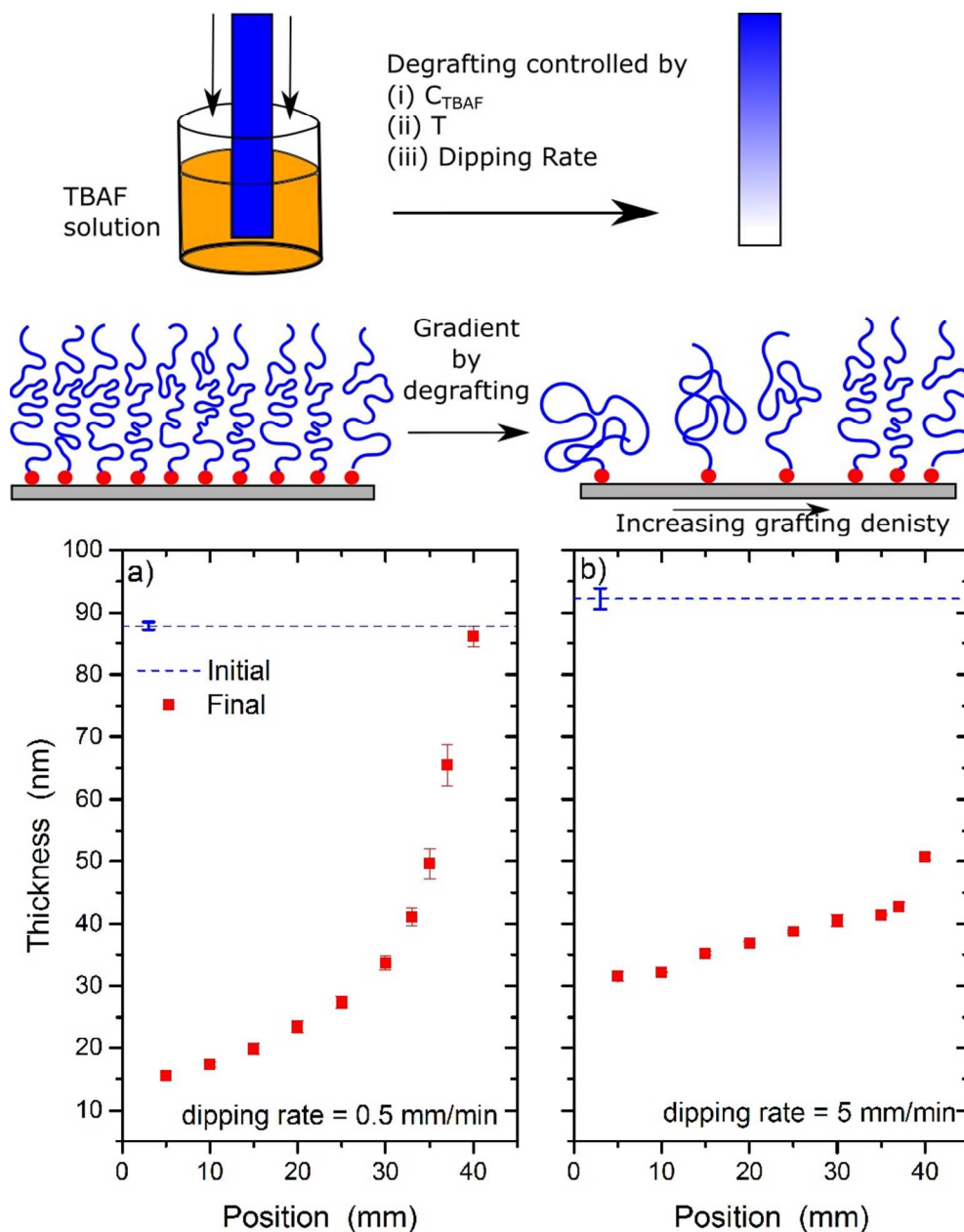


Figure 1. Dry thickness (h_p) of PMMA brushes plotted against the position on a substrate. Because the initial grafting density of PMMA was constant over the substrate the dry thickness change is a measure of the grafting density of PMMA brushes. Experimental conditions: a) $C_{\text{TBAF}}=0.1$ M, $T=40^\circ\text{C}$, dipping rate=0.5 mm/min. b) $C_{\text{TBAF}}=0.1$ M, $T=40^\circ\text{C}$, dipping rate=5.0 mm/min.

The grafting density and hence the corresponding dry thickness of the brush vary gradually across the sample. Such a substrate represents a true gradient in grafting density with constant polymer molecular weight since we begin with a uniform polymer brush layer with constant grafting density and molecular weight on the substrate. This technique is superior to creating grafting density gradients of brushes by a “conventional method”²⁹ which is based on depositing an inert silane layer using diffusion process and then backfilling the substrate with an initiator. In the conventional method, the polymer brush at different locations on the substrate grows under different degree of confinement, which may cause differences in the molecular weight and molecular weight polydispersity of the chains.³⁰ The dipping method also offers creating a desired grafting density gradient profile of the grafted polymer on the substrate by simply programming the dipping rate that corresponds to the desired profile assuming that the kinetics of degrafting is known. The ease of control is the key to having precision over the degrafting rate by TBAF.

2.2 Creating Other Polymer Brush Patterns

While the dipping method creates a continuous variation in the thickness, surface patterns with various in-plane shapes of polymer brushes can be created by delivering the TBAF solution to specific regions on the substrate. Using micro-contact printing, TBAF solution can be exposed using a hydrogel stamp with a desired shape. Here we used agarose as the hydrogel stamp material because it is not degraded by TBAF. An agarose stamp was soaked in 0.1 M TBAF solution in THF for 1 hr. The stamp was then brought in contact with a PMMA brush layer surface for 1 hr. The resulting pattern (mm scale) is visible to eye since the change in thickness changes the color of the polymer film. **Figures 2a-2c** show the initial substrate with polymer brush, the hydrogel stamp, and the substrate after stamping, respectively. **Figure 2d** shows patterns created by drying drops of TBAF solution. Optical microscopy images (**Figure 2e**) reveal that distinct regions on the surface are formed due to changing evaporation rate of the drop. The inner circle evaporated the latest; hence it will have the lowest grafting density and hence lowest thickness. **Figure 2f** shows an optical micrograph of the near interface region of one of the gradient sample (*cf.* **Figure 1b**) created using the dipping method explained earlier. The region to the left of the dotted line shows the gradation in color due to gradient in grafting density (and hence thickness) while the region to the right of the dotted line shows un-degrafted

polymer brush layer. In all these examples the incubation time and TBAF concentration can be varied to achieve greater control over the grafting density of the resulting pattern.

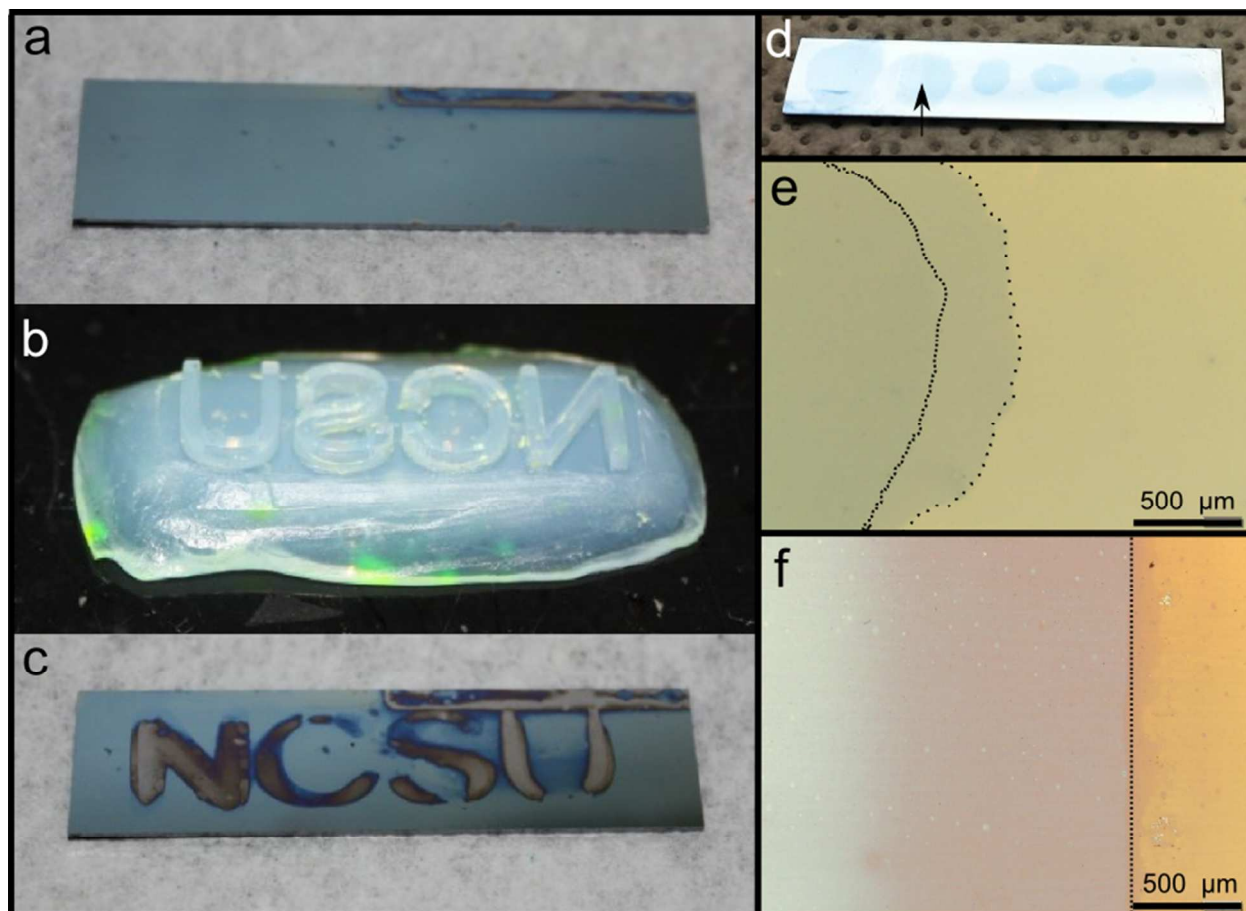


Figure 2. Surface pattern images on polymer brush containing substrate. a) Substrate coated with PMMA brush. b) Agarose hydrogel stamp with the desired pattern. c) Substrate after contact with TBAF-soaked agarose stamp; the grey regions have PMMA removed. d) Patterns of removed PMMA formed by depositing TBAF drops and letting them evaporate. e) Optical micrograph of the second drop from the left in d), the dotted line is drawn to guide the eyes and emphasize the different zones inside the drop. f) Optical micrograph of the region of the gradient sample where the gradient ends and un-grafted polymer brush region begins. The dotted line is drawn to separate the two regions. The dimensions of the substrates in a), c) and d) are 1 cm x 4.3 cm.

2.3 Reusability of Substrates

The low concentrations and incubation temperature during TBAF treatment ensure mild degrafting conditions so that the surface is not etched or damaged and is available for further and repeated modification. In **Figure 3** we plot thickness (h_p) and water contact angle (θ_{DIW}) for a

sequence of initiator deposition and PMMA brush growth steps before and after degrafting. The first eBMPUS layer (E1) was deposited by conventional method, *i.e.*, by first treating the substrate with ultraviolet ozone (UVO) treatment prior to the solution deposition of eBMPUS. The second and third initiator layers (E2 and E3) were deposited after degrafting PMMA and without any UVO treatment. PMMA brush was grown using ATRP as described in the Experimental section. Control samples (Control 1 and Control 2) were grown in the same reaction vessels but had eBMPUS layers deposited by conventional method, *i.e.*, by using UVO treatment prior to the initiator deposition. The results show that the thickness of the samples grown without any UVO treatment is comparable with that on samples prepared by the UVO-based conventional substrate treatment method. This is an important observation as it indicates: 1) complete removal of the organic layer via eBMPUS, which has been eluted to earlier,^{23,24} and 2) the ability of TBAF to activate the surface for attachment of organosilanes.

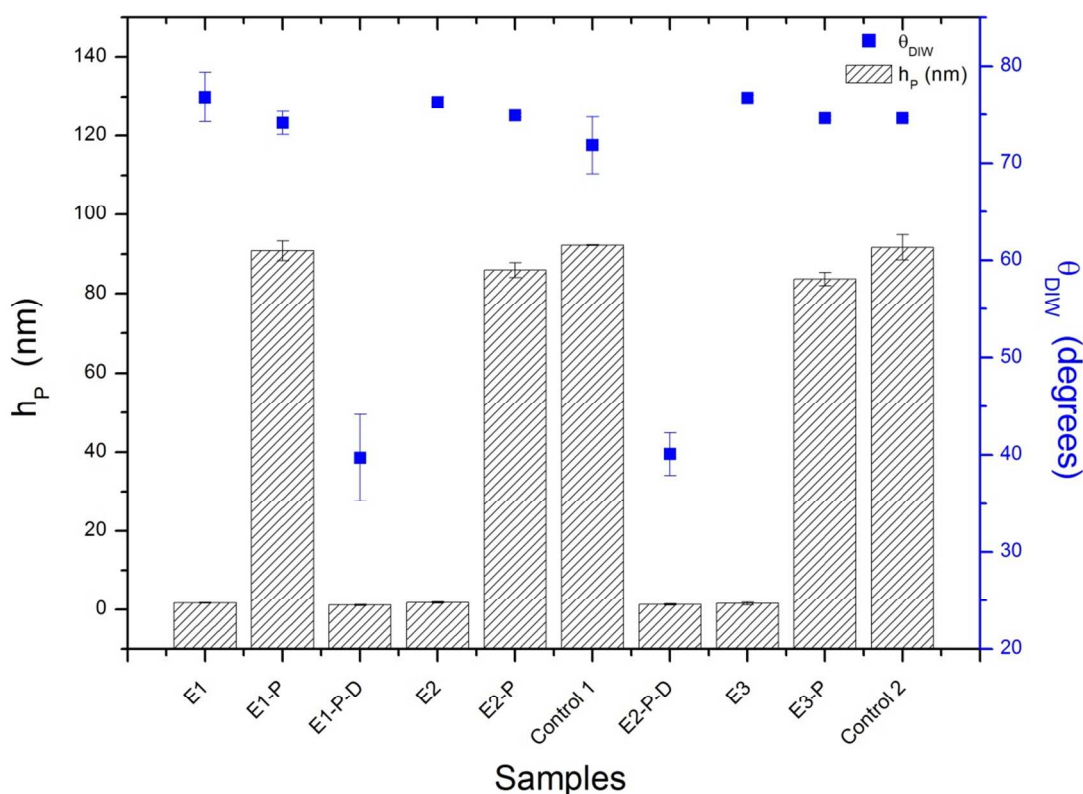


Figure 3. Dry ellipsometric thickness (h_p , bars) and water contact angle (θ_{DIW} , blue symbols) for repeated sequential deposition of eBMPUS (E) initiator and PMMA brush layer (P) grown after degrafting by ATRP. E1, E2, E3 refer to the first, second and third initiator deposition, respectively.

3.4 Re-growing polymer brushes without using UVO

We have shown previously that PMMA brushes can be degrafted from SiO_x substrates without any degradation and the collected PMMA can be analyzed using SEC to obtain molecular weight of the polymer.^{23,24} Here we demonstrate that the degrafted surface can be reused to deposit a second initiator layer which can then be employed to grow a different polymer brush layer. The second layer could be any polymer that can be grown by ATRP; here we first grow a polystyrene (PS) brush first followed by a PMMA brush. The X-ray photoelectron spectroscopy (XPS) data shown in **Figure 4** provide insight into chemical changes on the substrate during the technological steps involved in grafting/degrafting/regrafting. In addition, for each step we monitor the dry film thickness (h_p , solid symbols) and water contact angle (θ_{DIW} , open symbols). The starting substrate is a silicon wafer subjected to UVO treatment (data not shown), which cleans the surface from organic impurities and creates free hydroxyl groups needed for the attachment of the eBMPUS initiator molecules. The substrate is then covered with a monolayer of the eBMPUS initiator (black data). The silicon (Si 2p) and oxygen (O 1s) peaks (binding energies, BE, ~ 99 and ~ 534 eV, respectively) represent the underlying silica layer (~ 1 nm in thickness). The carbon (C 1s, BE ~ 285 eV) and bromine (Br 3d, BE ~ 70 eV) signals in the monolayer with $h_p = 1.6 \pm 0.1$ nm and $\theta_{DIW} = 77 \pm 2$ deg further confirm the presence of eBMPUS on the surface. A polystyrene (PS) brush (red data) with $h_p = 49 \pm 3$ nm is then grown from the initiator sites via ATRP. A strong carbon peak (BE ~ 285 eV) is detected in XPS but no silicon and oxygen peak are observed since the escape electrons from the underlying silica cannot reach the detector. The θ_{DIW} measured is 93 ± 2 deg, which is typical for PS. The high resolution XPS spectra show a characteristic aromatic peak in the C 1s peak at BE ~ 292 eV (see Supporting information). This PS polymer brush layer is then degrafted using 0.1 M TBAF at 50°C for 4 hrs. The green data in **Figure 4** correspond to the sample after TBAF degrafting. The Si 2p and O 1s peaks in the XPS data are visible again and the surface is hydrophilic with $\theta_{DIW} = 43 \pm 3$ deg. A monolayer of the eBMPUS ATRP initiator is subsequently deposited (blue) on this substrate but this time without exposing the substrate to UVO treatment. The C 1s and Br 3d peaks are detected in the XPS spectra and the θ_{DIW} increases to 73 ± 3 deg, close to the original eBMPUS monolayer (black data). PMMA layer of thickness 81 ± 2 nm ($\theta_{DIW} = 60 \pm 3$ deg) is then grown using ATRP (magenta). The high resolution C 1s peak in XPS for PMMA layer can be resolved

into its synthetic components; the ratio of their areas matches the stoichiometric ratio in PMMA (see Supporting information).

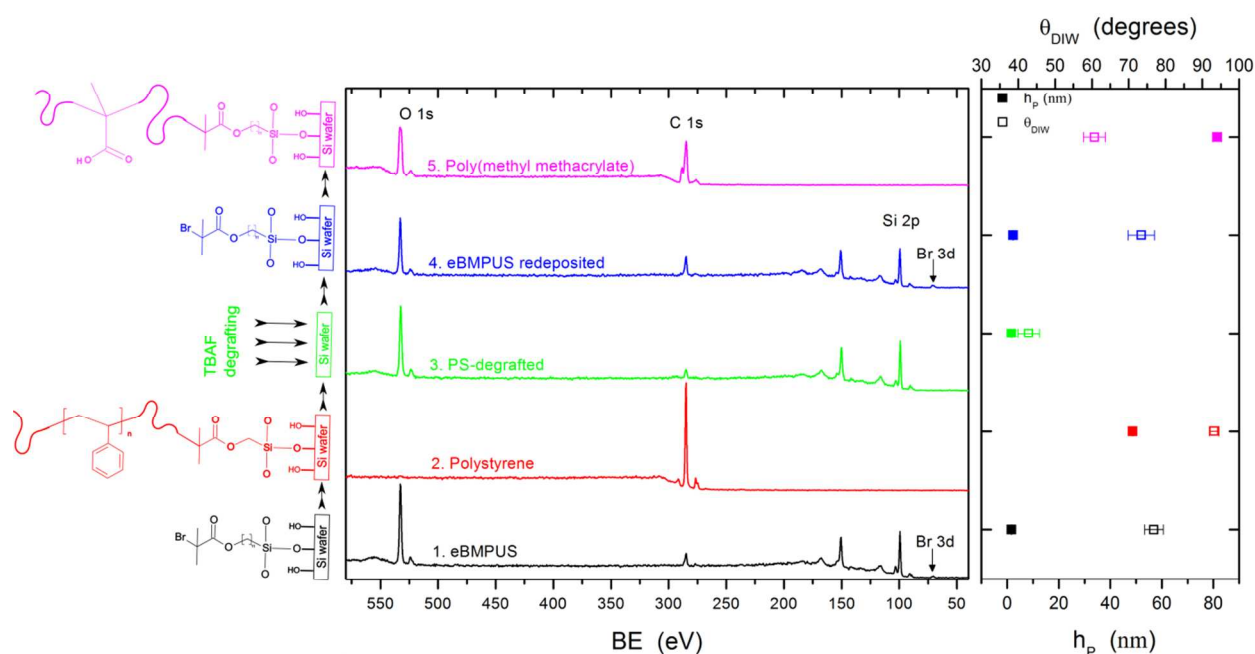


Figure 4. XPS scans for 5 different substrates, color coded with the cartoons on the left at different stages. The dry thickness (h_p , solid symbols) and water contact angle (θ_{DIW} , open symbols) are plotted on the right-side for the same 5 samples.

3.5 Degrafting of Half Substrate and Growing Diblock Copolymer on Other Half

One can degraft the polymer from selected sections on the substrate and re-growing a layer of a new polymer brush over the entire substrate. This procedure will lead to the formation of block copolymers (growth initiated from the remaining polymer brushes, which act as macroinitiators) and homopolymer brushes that grow from the degrafted regions of the substrate. To demonstrate this concept we first grow a PS brush (shown in red in **Figure 5**) from eBMPUS initiators by ATRP ($h_p=104.9 \pm 0.1$ nm and $\theta_{DIW}=95 \pm 2$ deg). A half of this substrate is then degrafted by incubating it in 0.1 M TBAF in THF at 50°C for 4 hrs resulting into half area available for new initiator deposition. This substrate is then incubated in eBMPUS solution followed by PMMA brush grown by ATRP for 24 hrs. Since there are ATRP active ends on the PS chains, a PS-*b*-PMMA diblock copolymer is grown on the PS covered area while the degrafted region is only decorated with PMMA homopolymer brushes. The thickness of diblock region was 158.9 ± 4 nm

($\theta_{DIW}=61 \pm 1$ deg) and the PMMA only region was measured as 124.8 ± 1.2 nm ($\theta_{DIW}=59 \pm 2$ deg). The substrate areas were characterized using FTIR. A carbonyl peak, characteristic for PMMA, observed at 1730 cm^{-1} , is detected in PMMA homopolymer and PS-PMMA diblock region while peaks corresponding to CH_2 deformation ($\sim 1460\text{ cm}^{-1}$), aromatic ring vibration ($\sim 1493\text{ cm}^{-1}$) and CH_2 rocking ($\sim 700\text{ cm}^{-1}$) for PS³¹ are observed in the PS homopolymer and PS-PMMA diblock copolymer region. The contact angle ($\theta_{DIW}=61 \pm 2$ deg) of the diblock region indicates that the PMMA block is present on the top of the PS brush.

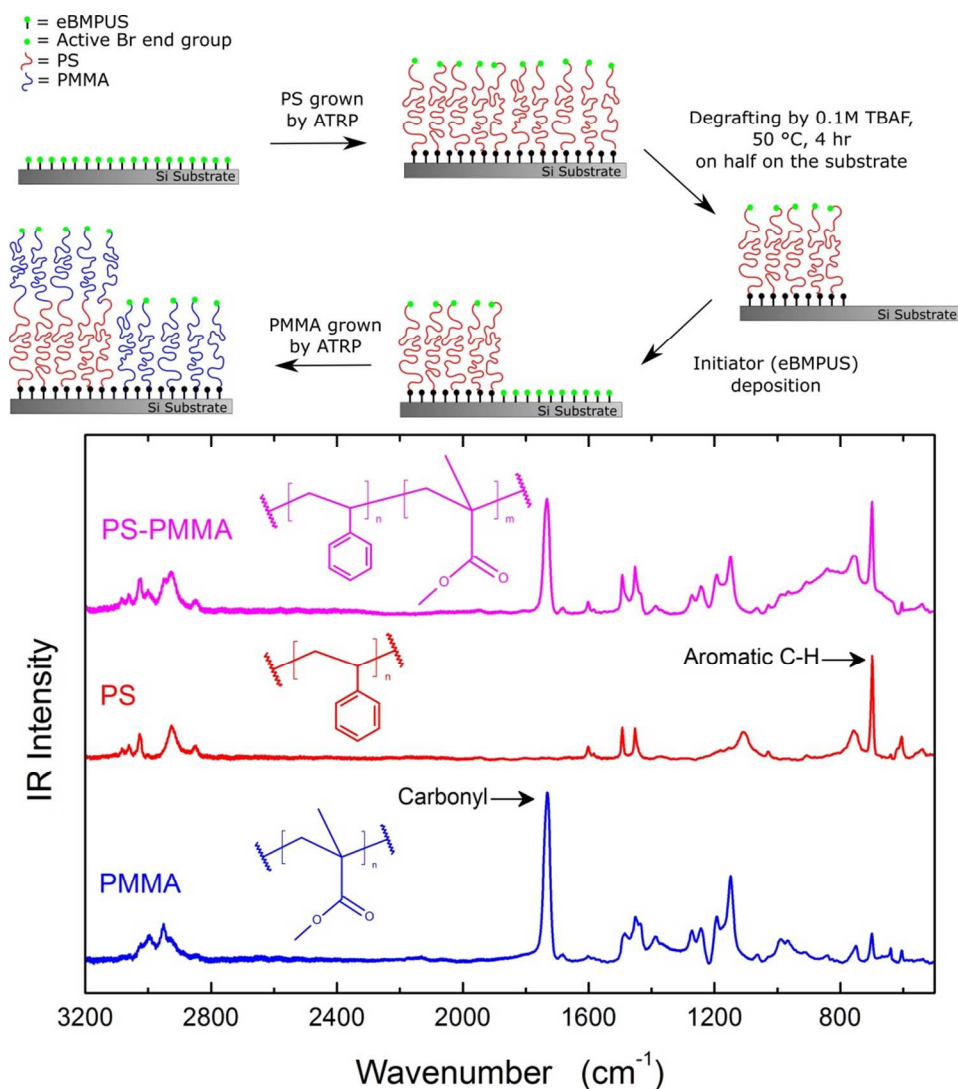


Figure 5. (Top) Scheme of creating a PMMA-PS diblock polymer brush on half of substrate while having PMMA only brush on the other half. (bottom) FTIR-spectra for PMMA region (blue), polystyrene only (red, control sample) and PS-PMMA diblock region (magenta).

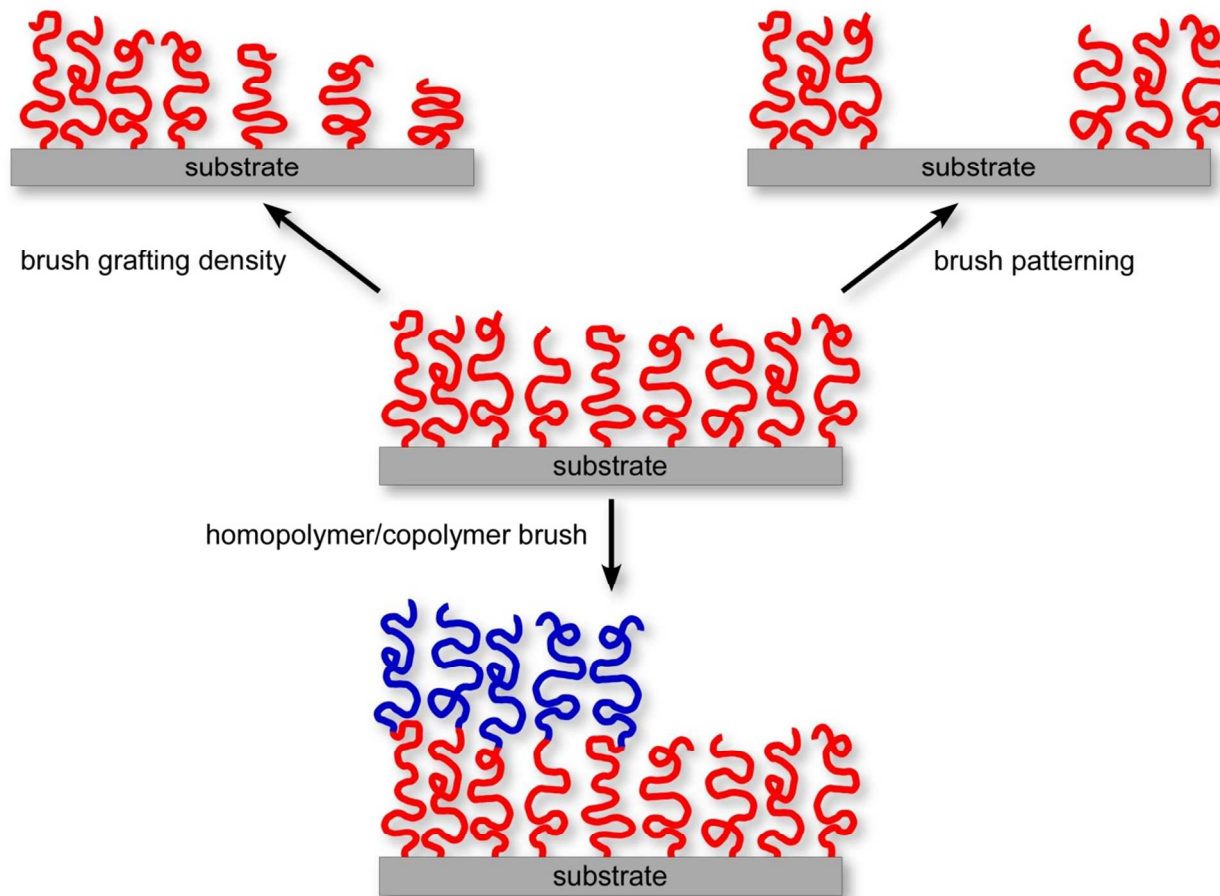
3. Conclusions

In this Communication we have shown that polymer brushes grown from silica-based substrates can be removed selectively by TBAF. The degrafted substrate can then be employed to grow a new polymer brush. This process can be repeated multiple times. The properties of the regrown brush layers are comparable to those prepared by conventional deposition method which employs UVO for surface activation needed or initiator attachment. A true gradient of grafting density for PMMA brushes can be created with degrafting by dipping method in TBAF solution. Spatial patterns of polymer brushes can be prepared by stamping of molded agarose hydrogel by microcontact printing. Combining the knowledge of the kinetics of degrafting and soft lithographic techniques facilitates creation of a brush patterns with good in-plane and out-of-plane control of grafting density and brush chemical composition.

Acknowledgements

We thank Dr. Jiří Šrogl for his contribution regarding understanding the chemistry of TBAF. The work was supported by the National Science Foundation (Grant no. DMR-1404639) and the Army Research Office under their Staff Research Program (Grant no. W911NF-04-D- 0003-0016).

TOC Figure



References

- 1 B. Zhao and W. J. Brittain, *Prog. Polym. Sci.*, 2000, **25**, 677–710.
- 2 P. G. de Gennes, *J. Phys.*, 1976, **37**, 1445–1452.
- 3 S. T. Milner, *Science*, 1991, **251**, 905–914.
- 4 D. M. Jones, J. R. Smith, W. T. S. Huck and C. Alexander, *Adv. Mater.*, 2002, **14**, 1130–1134.
- 5 Y. Li, J. Zhang, L. Fang, L. Jiang, W. Liu, T. Wang, L. Cui, H. Sun and B. Yang, *J. Mater. Chem.*, 2012, **22**, 25116–25122.
- 6 Y. Li, J. Zhang, W. Liu, D. Li, L. Fang, H. Sun and B. Yang, *ACS Appl. Mater. Interfaces*, 2013, **5**, 2126–2132.
- 7 X. Wang, R. Berger, J. I. Ramos, T. Wang, K. Koynov, G. Liu, H.-J. Butt and S. Wu, *RSC Adv.*, 2014, **4**, 45059–45064.
- 8 J. Hou, Q. Shi, W. Ye, Q. Fan, H. Shi, S. Wong, X. Xu and J. Yin, *ACS Appl. Mater. Interfaces*, 2014, **6**, 20868–20879.
- 9 J. Hou, Q. Shi, W. Ye, Q. Fan, H. Shi, S.-C. Wong, X. Xu and J. Yin, *Chem. Commun.*, 2015, **51**, 4200–4203.
- 10 L. Ionov, S. Minko, M. Stamm, J. F. Gohy, R. Jérôme and A. Scholl, *J. Am. Chem. Soc.*, 2003, **125**, 8302–8306.
- 11 I. Luzinov, S. Minko and V. V Tsukruk, *Prog. Polym. Sci.*, 2004, **29**, 635–698.
- 12 A. Kumar and G. M. Whitesides, *Appl. Phys. Lett.*, 1993, **63**, 2002–2004.
- 13 J. Genzer and R. R. Bhat, *Langmuir*, 2008, **24**, 2294–2317.
- 14 J. Genzer, *Annu. Rev. Mater. Res.*, 2012, **42**, 435–468.
- 15 B. Zhao, *Langmuir*, 2004, **20**, 11748–11755.
- 16 T. Chen, I. Amin and R. Jordan, *Chem. Soc. Rev.*, 2012, **41**, 3280–3296.
- 17 T. Chen, R. Jordan and S. Zauscher, *Polymer (Guildf.)*, 2011, **52**, 2461–2467.
- 18 T. Chen, R. Jordan and S. Zauscher, *Soft Matter*, 2011, **7**, 5532–5535.

- 19 T. Kamada, Y. Yamazawa, T. Nakaji-Hirabayashi, H. Kitano, Y. Usui, Y. Hiroi and T. Kishioka, *Colloids Surfaces B Biointerfaces*, 2014, **123**, 878–886.
- 20 H. J. Koo, K. V. Waynant, C. Zhang, R. T. Haasch and P. V. Braun, *Chem. Mater.*, 2014, **26**, 2678–2683.
- 21 C. Schuh, N. Lomadze, J. Rühle, A. Kopyshv and S. Santer, *J. Phys. Chem. B*, 2011, **115**, 10431–10438.
- 22 Q. Wei, B. Yu, X. Wang and F. Zhou, *Macromol. Rapid Commun.*, 2014, **35**, 1046–1054.
- 23 R. R. Patil, S. Turgman-Cohen, J. Šrogl, D. Kiserow and J. Genzer, *ACS Macro Lett.*, 2015, **4**, 251–254.
- 24 R. R. Patil, S. Turgman-Cohen, J. Šrogl, D. Kiserow and J. Genzer, *Langmuir*, 2015, **31**, 2372–2381.
- 25 T. von Werne and T. E. Patten, *J. Am. Chem. Soc.*, 1999, **121**, 7409–7410.
- 26 M. Kobayashi, M. Terada, Y. Terayama, M. Kikuchi and A. Takahara, *Macromolecules*, 2010, **43**, 8409–8415.
- 27 X. Jia, G. Zhang, W. Li, W. Sheng and C. Li, *J. Polym. Sci. Part A Polym. Chem.*, 2014, **52**, 1807–1814.
- 28 C. Kang, R. M. Crockett and N. D. Spencer, *Macromolecules*, 2014, **47**, 269–275.
- 29 M. K. Chaudhury and G. M. Whitesides, *Science*, 1992, **256**, 1539–1541.
- 30 S. Turgman-Cohen and J. Genzer, *Macromolecules*, 2010, **43**, 9567–9577.
- 31 C. Y. Liang and S. Krimm, *J. Mol. Spectrosc.*, 1959, **3**, 554–574.